Robotica (2009) volume 27, pp. 949–958. © Cambridge University Press 2009
doi:10.1017/S0263574709005372

Asymptotically stable biped gait generation based on stability principle of rimless wheel

Fumihiko Asano†* and Zhi-Wei Luo‡

†*School of Information Science, Japan Advanced Institute of Science and Technology, 1-1 Asahidai, Nomi, Ishikawa 923-1292, JAPAN*
‡*Department of Computer Science and Systems Engineering, Faculty of Engineering, Kobe University, 1-1 Rokkodai-cho, Nada-ku, Kobe 657-8501, JAPAN.*

(Received in Final Form: January 26, 2009. First published online: March 6, 2009)

SUMMARY
We investigated and identified the conditions necessary for stable dynamic gait generation in biped robots from the mechanical energy balance point of view. The equilibrium point at impact in a dynamic gait is uniquely determined by two conditions; keeping the restored mechanical energy constant and settling the relative hip-joint angle to the desired value before impact. The generated gait then becomes asymptotically stable around the equilibrium point determined by these conditions. This is shown by a simple recurrence formula of the kinetic energy immediately before impact. We verified this stability theorem using numerical simulation of virtual passive dynamic walking. The results were compared with those for a rimless wheel and an inherent stability principle was derived. Finally, we derived a robust control law using a reference mechanical energy trajectory and demonstrated its effectiveness numerically.

KEYWORDS: Gait generation; Biped robot; Asymptotic stability; Mechanical energy balance; Virtual passive dynamic walking.

1. Introduction

Elucidating the stability of a dynamic gait is a basic problem in the study of limit cycle walkers. Passive-dynamic walkers[1] exhibit stable dynamic walking without any control, but it is unclear how gait stability is achieved. Analyzing and understanding the stability of limit cycles with impacts is difficult because of the complexity of the nonlinear hybrid dynamical system. It has been empirically shown that a stable dynamic gait with impacts can be synthesized by adjusting the parameters of walking system.

Several earlier studies took limit cycle stability into account.[2–4] Doing so required precise design of the desired trajectories or adjustment of the system parameters. Several approaches to stability analysis have more recently been taken. Goswami *et al.* used the Poincaré return map to analyze the stability of passive compass gaits.[5] They numerically calculated the Jacobian matrix of the return map using four simulation tests. Asano *et al.* adopted this approach and reduced the dimension of the return map to three.[6] With these approaches, however, the existence of a stable one-periodic gait must be assumed. Garcia *et al.* analytically discussed the basin of attraction using the simplest walking model.[7] Their approach, however, is limited to walking models for which the leg mass can be neglected.

Several methods for analyzing stability without assuming a stable limit cycle have been proposed. Hosoe *et al.*[8] and Grizzle *et al.*[9] investigated the stability of the planar dynamic bipedal gait by using the Poincaré return map. They reduced the number of the degrees of freedom (DOF) in the walking system by using high-gain feedback or deadbeat control, so the walking system could be regarded as a one-link rigid body. They needed at least two numerical simulation tests for drawing the approximated return map. Ikemata *et al.* investigated the limit cycle stability of the simplest walking model using the reduced Poincaré return map and showed that the generated gait is always asymptotically stable if the impact posture is fixed.[10] A related result was also reported by Wisse *et al.*,[11] and they observed that the stability mechanism is equivalent to that of a rimless wheel. Although a constraint condition on the impact posture is common to all these works, the results differed, and the reason has not been clarified.

We have investigated the gait stability of limit cycle walkers from the viewpoint of mechanical energy balance. Dynamic walking cycles are generated by restoring mechanical energy lost by heel strikes,[6] and the magnitude of the restored energy converges to that of the dissipated energy in a steady gait. In other words, balanced mechanical energy creates a stable dynamic gait. We identified the conditions necessary to systematically achieve this energy balance and clarified their physical meanings. We then developed a simple planar compass-like biped model and trajectory tracking control for the hip-joint angle and, using a simple recurrence formula of the kinetic energy immediately before impact, we demonstrated asymptotic stability around the equilibrium point. The validity of this approach was proven for gait generation using a virtual passive dynamic walking.[6] Only one simulation test was required to detect whether the gait was stable or not. Although there is an alternative approach to generating stable gaits based on mechanical energy considering global stability,[12] we focused

* Corresponding author. E-mail: fasano@jaist.ac.jp

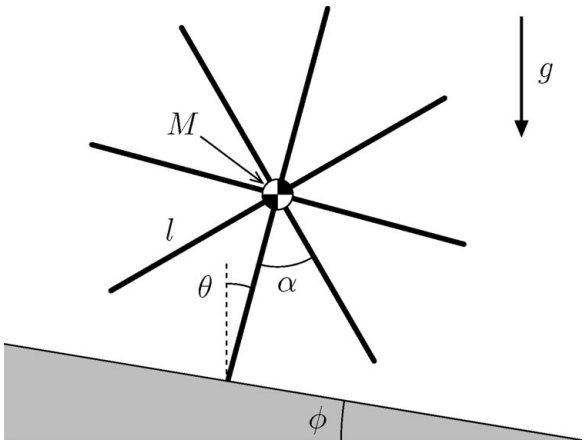

Fig. 1. Rimless wheel model.

on forward dynamic walking. The generated gait was shown to be essentially as stable as a virtual rimless wheel.

2. Two Simple Walking Models

Before discussing the main problem, this section introduces two simple walking models to clarify the key mechanisms of asymptotic stability.

2.1. Rimless wheel model

Figure 1 shows a model of a rimless wheel. We assume that this model has a point mass of M (kg) at the central position and consists of massless legs whose length is l (m). We also assume that the impact of each leg with the ground is inelastic without sliding or slipping. Given a suitable initial condition, the rimless wheel rolls down a slope, and the rolling pattern converges to one-periodic stable limit cycle if the next collision always occurs. This stability mechanism is explained as follows.

Let θ (rad) be the angular position of a leg contacting the ground with respect to the vertical direction as shown in Fig. 1. We assume that it switches to the next contacting leg after impact. The angular velocity relationship between immediately before and immediately after impact is given by

$$\dot{\theta}^+ = \cos\alpha \cdot \dot{\theta}^-, \tag{1}$$

where α (rad) is the interleg angle, as shown in Fig. 1. The kinetic energy then has the following simple relationship between immediately after and immediately before impact:

$$K^+ = \frac{1}{2}Ml^2(\dot{\theta}^+)^2 = \frac{1}{2}Ml^2(\cos\alpha \cdot \dot{\theta}^-)^2 = \cos^2\alpha \cdot K^- \tag{2}$$

The energy-loss coefficient ε (-), which is defined as

$$\varepsilon := \frac{K^+}{K^-} = \cos^2\alpha, \tag{3}$$

is kept constant. The restored mechanical energy during one step ΔE (J) is also kept constant

$$\Delta E = 2Mgl \sin\frac{\alpha}{2}\sin\phi. \tag{4}$$

Since the $(i+1)$th kinetic energy immediately before impact is determined by the sum of the ith kinetic energy immediately after impact and the restored mechanical energy, we can obtain the recurrence formula

$$K^-[i+1] = K^+[i] + \Delta E, \tag{5}$$

where i is the number of steps. For all i, the relationship

$$K^+[i] = \varepsilon K^-[i] \tag{6}$$

holds, and, by substituting this into Eq. (5), we get

$$K^-[i+1] = \varepsilon K^-[i] + \Delta E. \tag{7}$$

This is a function of K^- only. ε and ΔE are constants. We can thus solve Eq. (7) for $K^-[i]$, i.e. the general term

$$K^-[i] = \frac{\Delta E}{1-\varepsilon} + \varepsilon^i\left(K^-[0] - \frac{\Delta E}{1-\varepsilon}\right). \tag{8}$$

This leads to

$$K^-_* := \lim_{i\to\infty} K^-[i] = \frac{\Delta E}{1-\varepsilon}, \tag{9}$$

which proves asymptotic stability. This mechanism was also investigated by Tazaki and Imura.[13] In addition, Coleman also analyzed the mechanism in detail from the viewpoints of Poincaré return map and energetics.[14] He did not use the simple recurrence formula of kinetic energy, but succeeded in the approximate proof of asymptotic stability.

2.2. Simplest walking model

The simplest walking model, shown in Fig. 2, is a planar compass-like biped model[7] consisting of three point masses. The hip mass is sufficiently larger than the leg mass ($m_H \gg m$), and the leg masses are positioned at the tips of the legs. The dynamic equation and transition equation are thus very simple, and the swing-leg motion immediately before impact does not affect the angular velocity immediately after impact. The Poincaré return map is also simplified and can be defined as a function of the angular velocity immediately before impact of the stance leg and the relative hip angle.

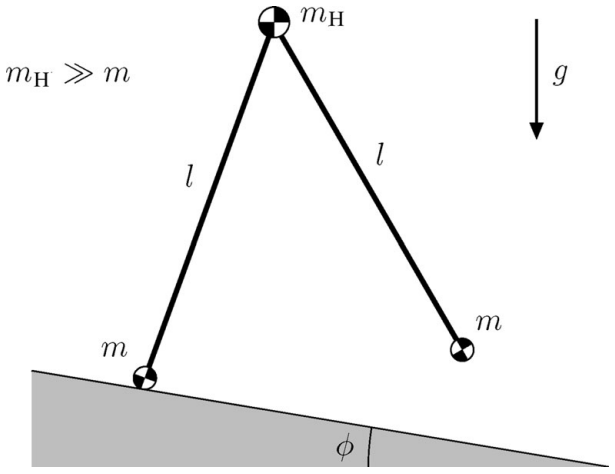

Fig. 2. Simplest walking model.

Ikemata *et al.* used this model to investigate the stability principle and showed that the generated dynamic gait is always asymptotically stable if the relative hip angle is kept constant.[10] They derived the eigenvalues of the Poincaré return map for when the relative hip angle at impact is constant. If α (rad) is the relative hip angle at impact, the eigenvalues yield $\cos^2\alpha$ and 0. The same result was also found by Wisse *et al.*[11] who also observed that the simplest walking model follows the same stability principle as the rimless wheel model. This is because the stance leg exchange in this walking model is performed in the same manner, so the energy-loss coefficient and restored mechanical energy are inherently constant in accordance with the relative hip angle at impact if every impact posture is the same. In other words, the simplest walking model discretely behaves in the same manner as the rimless wheel model if α is constant. In this sense, the results by Ikamata *et al.* and Wisse *et al.* are obvious, and provide a new understanding of the results of Tazaki and Imura.[13] See the Appendix for a detailed analysis.

Here, we describe a more general case of a biped model regarding its leg mass.

3. Problem Formulation

3.1. Model of compass-like biped robot

As shown in Fig. 3, the model of a planar, fully-actuated, compass-like biped robot with flat feet has two joint torques u_1 and u_2 that can be exerted at the ankle joint and hip joint. As we described in a previous paper,[15] semicircular feet are well suited for energy-efficient and high-speed biped locomotion, but full actuation is necessary to satisfy the conditions necessary for stable gait generation, as described later. Let $\boldsymbol{\theta} = [\theta_1\ \theta_2]^{\mathrm{T}}$ be the generalized coordinate vector, where θ_1 and θ_2 are the angular positions of the stance and swing legs with respect to vertical. The dynamic equation

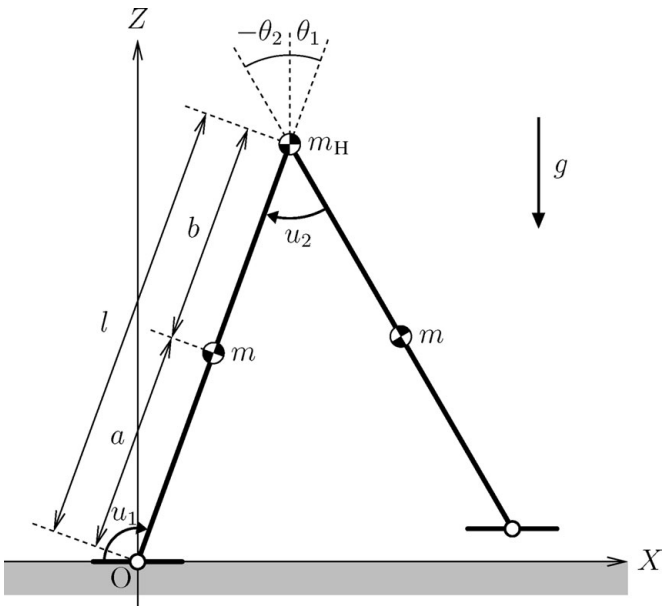

Fig. 3. Model of planar, fully actuated, compass-like biped robot.

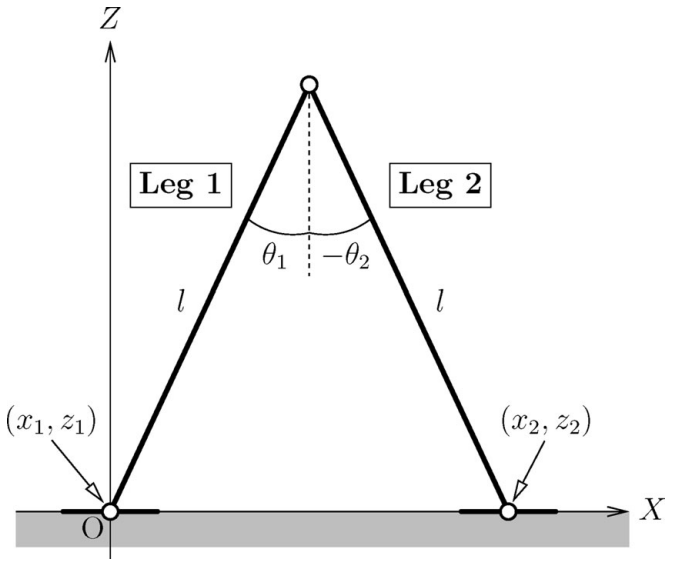

Fig. 4. Configuration at instant of heel strike.

then yields

$$\boldsymbol{M}(\boldsymbol{\theta})\ddot{\boldsymbol{\theta}} + \boldsymbol{C}(\boldsymbol{\theta}, \dot{\boldsymbol{\theta}})\dot{\boldsymbol{\theta}} + \boldsymbol{g}(\boldsymbol{\theta}) = \boldsymbol{S}\boldsymbol{u} = \begin{bmatrix} 1 & 1 \\ 0 & -1 \end{bmatrix} \begin{bmatrix} u_1 \\ u_2 \end{bmatrix}. \quad (10)$$

These matrices are described in detail elsewhere.[6] If we assume inelastic collisions for the stance-leg exchange and set suitable values for the physical parameters, the robot can exhibit passive dynamic walking on a gentle slope. Let E be the total mechanical energy of the robot, and relationship $\dot{E} = \dot{\boldsymbol{\theta}}^{\mathrm{T}}\boldsymbol{S}\boldsymbol{u}$ between the mechanical energy and the control inputs holds.

The modeling of an inelastic collision is briefly described here. A more detailed explanation is given elsewhere.[15] We extended the configuration as shown in Fig. 4. We define the stance and swing legs immediately before impact as "Leg 1" and "Leg 2" and derive their dynamic models independently. We define $\boldsymbol{q}_i = [x_i\ z_i\ \theta_i]^{\mathrm{T}}$ as the extended coordinate vector for Leg i and define $\boldsymbol{q} = [\boldsymbol{q}_1^{\mathrm{T}}\ \boldsymbol{q}_2^{\mathrm{T}}]^{\mathrm{T}}$ as that of the whole system. The inelastic collision model is then derived as

$$\bar{\boldsymbol{M}}(\boldsymbol{q})\dot{\boldsymbol{q}}^{+} = \bar{\boldsymbol{M}}(\boldsymbol{q})\dot{\boldsymbol{q}}^{-} - \boldsymbol{J}_I(\boldsymbol{q})^{\mathrm{T}}\boldsymbol{\lambda}_I, \quad (11)$$

where $\bar{\boldsymbol{M}} \in \mathbb{R}^{6\times 6}$ is the inertia matrix corresponding to $\boldsymbol{q}$, and superscripts "+" and "−" respectively stand for immediately after and immediately before impact. The $\boldsymbol{J}_I(\boldsymbol{q}) \in \mathbb{R}^{4\times 6}$ is the Jacobian matrix derived from the geometric constraint conditions at the instant of heel strike; it should satisfy the following velocity constraint condition immediately after impact:

$$\boldsymbol{J}_I(\boldsymbol{q})\dot{\boldsymbol{q}}^{+} = \boldsymbol{0}_{4\times 1}. \quad (12)$$

The detailed derivation of $\boldsymbol{J}_I(\boldsymbol{q})$ and $\boldsymbol{\lambda}_I \in \mathbb{R}^4$ as the Lagrange undetermined multiplier vector representing the impact force is described elsewhere.[15]

3.2. Constraint control of impact posture

Previous methods for gait stability analysis simplified the walking system by assuming a contact robot posture

immediately prior to every heel strike.[8–10] Reducing the number of DOF or regarding the robot dynamics to be that of a one-link rigid body facilitates analysis of the walking system. For the compass-like biped model in Fig. 3, this condition is achieved by simply adjusting the relative hip-joint angle, $\theta_{\rm H} := \theta_1 - \theta_2$, to the desired one, $\theta_{\rm H}^*$, immediately prior to each heel strike. As described later, we achieve this condition by introducing a time-dependent desired trajectory for the hip-joint angle. We further assume that this control is always completed before the heel strikes. A compass gait with this constraint control on the impact posture is termed as "constrained compass gait." It is described in detail in Section 6.

4. Definitions and Theorem for Asymptotically Stable Gait

This section defines the basic parameters, terms, and their notations used for generating an asymptotically stable bipedal gait. It also introduces the theorem for an asymptotically stable gait.

4.1. Basic definitions

Definition 1. *Time interval T (s), which is the interval from the instant of one stance-leg exchange to the next, is called the "step period."*

Definition 2. *The robot starts walking from the impact posture shown in Fig. 4 at* 0 *(s); this is defined as the zeroth collision. The next heel-strike collision is the first collision, and the motion between the zeroth and the first collisions is called the "first step". The subsequent collisions and steps are contextually counted.*

Definition 3. *Let $T_{\rm set}$ (s) be the desired settling-time for trajectory tracking control of the hip joint. We assume that $T \geq T_{\rm set}$ holds in successful walking. This is called the "settling-time condition."*

Definition 4. *Let $\Delta E := E(T^-) - E(0^+)$ (J) be the restored mechanical energy by control inputs during one cycle. It is called the "restored mechanical energy."*

4.2. Theorem of asymptotically stable gait

We need to consider two lemmas before discussing the main theorem.

Lemma 1. *If the following two conditions hold, the equilibrium points of the constrained compass gait are systematically determined.*

Condition 1 *ΔE is constant for every step.*

Condition 2 *The next heel-strike collision occurs under the settling-time condition.*

Lemma 2. *The energy loss coefficient remains constant given Condition 2.*

Then the following theorem holds.

Theorem 1. *A generated constrained compass gait is asymptotically stable under Conditions 1 and 2.*

We give the proof of Lemmas 1 and 2 in the following sections.

5. Generation of Equilibrium Points Based on Mechanical Energy Balance

This section describes the mechanism of mechanical energy balance in a dynamic gait and discusses how the equilibrium points in a dynamic gait are systematically generated.

5.1. Dissipated energy

We define the total energy dissipated by heel strikes as

$$\Delta E_{\rm hs} := \frac{1}{2}(\dot{\boldsymbol{q}}^+)^{\rm T}\bar{\boldsymbol{M}}(\boldsymbol{q})\dot{\boldsymbol{q}}^+ - \frac{1}{2}(\dot{\boldsymbol{q}}^-)^{\rm T}\bar{\boldsymbol{M}}(\boldsymbol{q})\dot{\boldsymbol{q}}^- \leq 0, \quad (13)$$

which is equal to dissipated kinetic energy because the potential energy does not change at the instant of a heel strike. This equation can be rearranged as follows. Equations (11) and (12) show that the velocity immediately after impact $\dot{\boldsymbol{q}}^+$ yields $\dot{\boldsymbol{q}}^+ = \boldsymbol{Y}\dot{\boldsymbol{q}}^-$, where

$$\boldsymbol{Y} := \boldsymbol{I}_6 - \bar{\boldsymbol{M}}^{-1}\boldsymbol{J}_I^{\rm T}\left(\boldsymbol{J}_I\bar{\boldsymbol{M}}^{-1}\boldsymbol{J}_I^{\rm T}\right)^{-1}\boldsymbol{J}_I. \quad (14)$$

The relationship $\dot{\boldsymbol{q}}^- = \boldsymbol{H}\dot{\boldsymbol{\theta}}^-$ holds for the velocity immediately before impact. By using this relationship, we can simplify $\Delta E_{\rm hs}$

$$\Delta E_{\rm hs} = -\frac{1}{2}(\dot{\boldsymbol{\theta}}^-)^{\rm T}\boldsymbol{N}\dot{\boldsymbol{\theta}}^- \leq 0, \quad (15)$$

$$\boldsymbol{N} := \boldsymbol{H}^{\rm T}\boldsymbol{J}_I^{\rm T}\left(\boldsymbol{J}_I\bar{\boldsymbol{M}}^{-1}\boldsymbol{J}_I^{\rm T}\right)^{-1}\boldsymbol{J}_I\boldsymbol{H}. \quad (16)$$

The details of matrices $\boldsymbol{H} \in \mathbb{R}^{6\times 2}$ and $\boldsymbol{N} \in \mathbb{R}^{2\times 2}$ are described later. They are simply function matrices of the hip-joint angle $\theta_{\rm H}^*$ at the instant of a heel strike in a constrained compass gait. If K is the kinetic energy, $\Delta E_{\rm hs} = K^+ - K^- \leq 0$, i.e. $K^+ \leq K^-$. This is because kinetic energy always dissipates in inelastic collisions.

5.2. Condition of mechanical energy balance

Let the restored mechanical energy ΔE be constant. It is then equal to the magnitude of the dissipated energy, and

$$\Delta E = \frac{1}{2}(\dot{\boldsymbol{\theta}}^-)^{\rm T}\boldsymbol{N}(\theta_{\rm H}^*)\dot{\boldsymbol{\theta}}^- = -\Delta E_{\rm hs} \quad (17)$$

holds. This is an ellipse in the configuration space of the angular velocities immediately before impact, the $\dot{\theta}_1^-$–$\dot{\theta}_2^-$ plane. It is expressed as

$$N_{11}(\dot{\theta}_1^-)^2 + 2N_{12}\dot{\theta}_1^-\dot{\theta}_2^- + N_{22}(\dot{\theta}_2^-)^2 = 2\Delta E, \quad (18)$$

where N_{ij} is the (i, j) component of matrix $\boldsymbol{N}$.

$$\boldsymbol{N}(\theta_{\rm H}^*) = \begin{bmatrix} N_{11} & N_{12} \\ N_{12} & N_{22} \end{bmatrix}$$

$$N_{11} = \Delta_N(1 + \beta^2 + (2\beta^2 - 2\beta + 3)\gamma + \gamma^2 - (1 + \gamma + (\beta + \gamma)^2)\cos(2\theta_{\rm H}^*))$$

$$N_{12} = \Delta_N(1 - \beta)(-1 - 2(1 - \beta)\gamma + \cos(2\theta_{\rm H}^*))\cos\theta_{\rm H}^*$$

$$N_{22} = \Delta_N(1 - \beta)^2(1 + 2\gamma - \cos(2\theta_{\rm H}^*))$$

$$\Delta_N = ml^2/(1 + 2\beta^2 + 2\gamma - \cos(2\theta_{\rm H}^*)),$$

Table I. Parameter settings for walking system.

m	5.0 (kg)	ϕ	0.02 (rad)
m_{H}	10.0 (kg)	θ_{H}^*	0.40 (rad)
l	1.00 (m)	k_{d}	100 (s^{-1})
a	0.50 (m)	k_{p}	2500 (s^{-2})

where $\beta := a/l$ (-) is the location of leg's CoM position, and $\gamma := m_{\mathrm{H}}/m$ is the mass ratio. The shape of the ellipse is uniquely determined by the restored mechanical energy ΔE and desired hip-joint angle θ_{H}^*. Figure 5 shows the ellipse when $\Delta E = 1.50$ (J) and the robot's physical parameters are set as shown in Table I. If constraint control of impact posture is achieved or condition $\dot{\theta}_1^- = \dot{\theta}_2^-$ holds, the equilibrium points are uniquely and systematically determined.

By substituting $\dot{\theta}_1^- = \dot{\theta}_2^- = \dot{\theta}_*^-$ into Eq. (18), we obtain

$$\dot{\theta}_*^- = \pm\sqrt{\frac{2\Delta E}{N_{11} + 2N_{12} + N_{22}}}. \tag{19}$$

Here, we deal only with the equilibrium point in the first quadrant, i.e. the case of walking forward. That in the third quadrant implies walking backward with the same motion. The ellipse enlarges with an increase in ΔE, i.e. the walking speed increases as ΔE is increased.

6. Asymptotic Stability

This section describes the asymptotic stability of a constrained compass gait and discusses its similarity to that of a rimless wheel.

6.1. Energy loss coefficient

If $\theta_{\mathrm{H}}^- = \theta_{\mathrm{H}}^*$ is achieved by constraint control of the impact posture, the following relationship for the velocities immediately before impact holds:

$$\dot{\boldsymbol{q}}^- = \boldsymbol{H}\dot{\boldsymbol{\theta}}^- = \boldsymbol{H}\begin{bmatrix}1\\1\end{bmatrix}\dot{\theta}_1^- \tag{20}$$

The angular velocity vector immediately before impact can then be simply expressed using $\dot{\theta}_1^-$

$$\dot{\boldsymbol{\theta}}^+ = \begin{bmatrix}0&0&0&0&0&1\\0&0&1&0&0&0\end{bmatrix}\boldsymbol{Y}\boldsymbol{H}\begin{bmatrix}1\\1\end{bmatrix}\dot{\theta}_1^- =: \boldsymbol{\xi}\dot{\theta}_1^-, \tag{21}$$

where $\boldsymbol{H} = \boldsymbol{H}(\theta_{\mathrm{H}}^*) \in \mathbb{R}^{6\times 2}$ and $\boldsymbol{\xi} = \boldsymbol{\xi}(\theta_{\mathrm{H}}^*) \in \mathbb{R}^2$ are function matrices.

$$\boldsymbol{H}(\theta_{\mathrm{H}}^*) = \begin{bmatrix} 0 & 0 \\ 0 & 0 \\ 1 & 0 \\ l\cos\dfrac{\theta_{\mathrm{H}}^*}{2} & -l\cos\dfrac{\theta_{\mathrm{H}}^*}{2} \\ -l\sin\dfrac{\theta_{\mathrm{H}}^*}{2} & -l\sin\dfrac{\theta_{\mathrm{H}}^*}{2} \\ 0 & 1 \end{bmatrix} \tag{22}$$

$$\boldsymbol{\xi}(\theta_{\mathrm{H}}^*) = \begin{bmatrix} \dfrac{-2\left(\beta(1-\beta)-(\beta+\gamma)\cos\theta_{\mathrm{H}}^*\right)}{1+2\beta^2+2\gamma-\cos\left(2\theta_{\mathrm{H}}^*\right)} \\ \dfrac{\gamma-2\beta(\beta^2+\gamma)-2(1-\beta)\beta\cos\theta_{\mathrm{H}}^*+(2\beta+\gamma)\cos\left(2\theta_{\mathrm{H}}^*\right)}{(1-\beta)\left(1+2\beta^2+2\gamma-\cos\left(2\theta_{\mathrm{H}}^*\right)\right)} \end{bmatrix} \tag{23}$$

Note that $\boldsymbol{\xi}$ does not depend on the leg length or mass. The inertia matrix of a compass-like biped on the other hand is

$$\boldsymbol{M}(\boldsymbol{\theta}) = \begin{bmatrix} m_{\mathrm{H}}l^2 + ma^2 + ml^2 & -mbl\cos\theta_{\mathrm{H}} \\ -mbl\cos\theta_{\mathrm{H}} & mb^2 \end{bmatrix}, \tag{24}$$

and this can be considered equivalent to $\boldsymbol{M} = \boldsymbol{M}(\theta_{\mathrm{H}})$.

Using these matrices and vectors, we can express the kinetic energy immediately after impact as

$$K^+ = \frac{1}{2}\boldsymbol{\xi}^{\mathrm{T}}\boldsymbol{M}(-\theta_{\mathrm{H}}^*)\boldsymbol{\xi}(\dot{\theta}_1^-)^2 =: \frac{1}{2}\bar{M}^+(\dot{\theta}_1^-)^2 \tag{25}$$

and that immediately before impact as

$$K^- = \frac{1}{2}\begin{bmatrix}1\\1\end{bmatrix}^{\mathrm{T}}\boldsymbol{M}(\theta_{\mathrm{H}}^*)\begin{bmatrix}1\\1\end{bmatrix}(\dot{\theta}_1^-)^2 =: \frac{1}{2}\bar{M}^-(\dot{\theta}_1^-)^2. \tag{26}$$

Note that $\boldsymbol{M}(\theta_{\mathrm{H}}^*) = \boldsymbol{M}(-\theta_{\mathrm{H}}^*)$. Using these equations, we define the energy loss coefficient as

$$\varepsilon := \frac{K^+}{K^-} = \frac{\bar{M}^+}{\bar{M}^-}. \tag{27}$$

Both $\bar{M}^+$ and $\bar{M}^-$ depend only on θ_{H}^*, so ε is constant. This is a dimensionless quantity, and we can find $0 < \varepsilon < 1$ because $0 < K^+ < K^-$.

6.2. Asymptotic stability

If ΔE is constant, the following recurrence formula for the kinetic energy at impact between the $(i+1)$th and the ith

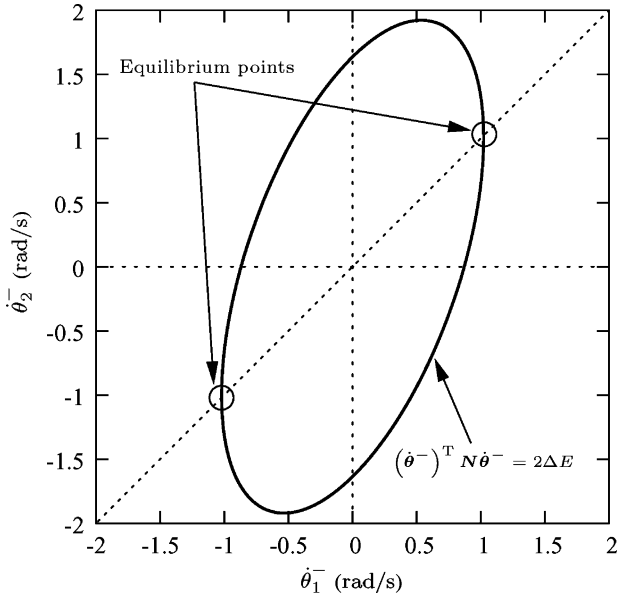

Fig. 5. Ellipse of angular velocities immediately before impact and equilibrium points determined by mechanical energy balance and constraint on impact posture, where $\Delta E = 1.50$ (J).

steps holds:

$$K^-[i+1] = K^+[i] + \Delta E. \tag{28}$$

The relationship $K^+[i] = \varepsilon K^-[i]$ holds for all i, and, by substituting it into Eq. (28), we obtain a simple recurrence formula for K^-,

$$K^-[i+1] = \varepsilon K^-[i] + \Delta E, \tag{29}$$

which shows that the walking system is asymptotically stable in the same manner as a rimless wheel. As such, the generated bipedal gait should be termed the "virtual rimless wheel gait." From Eqs. (26) and (29), we obtain the recurrence formula for $\dot{\theta}_1^-[i]$:

$$\dot{\theta}_1^-[i+1] = \sqrt{\varepsilon\left(\dot{\theta}_1^-[i]\right)^2 + \frac{2\Delta E}{\bar{M}^-}}. \tag{30}$$

The equilibrium point of Eq. (30) $\dot{\theta}_*^-$ is also found to be asymptotically stable from the geometric relationship between the parabola and the 45° line. This is described in detail in the next section.

Here we deal only with a simple compass-like biped for simplicity. Nevertheless, the obtained results are applicable to all biped robots, regardless of their DOF, that have the same posture as a 1-DOF rigid body under the two constraint conditions previously mentioned.

7. Validation Using Virtual Passive Dynamic Walking

Now that we have clarified the conditions necessary for asymptotically stable gait generation, we can validate Theorem 1 using a virtual passive dynamic walking model that satisfies Condition 1 for a given θ_{H}^*.

7.1. Theorem 1 validation

The simplest way to uniquely determine ΔE for a given θ_{H}^* is to use a virtual passive dynamic walking (VPDW) model,[6] which is used to generate a level gait with virtual gravity as the driver. The following relationship between the total mechanical energy and the X-position of CoM, X_g, holds in VPDW:

$$\frac{\partial E}{\partial X_g} = Mg\tan\phi, \tag{31}$$

where $M := m_{\mathrm{H}} + 2m$ (kg) is the robot's total mass, and ϕ (rad) is the virtual slope angle. Taking into account $\dot{E} = \dot{\boldsymbol{\theta}}^{\mathrm{T}}\boldsymbol{S}\boldsymbol{u}$, we can expand Eq. (31)

$$\dot{E} = \dot{\theta}_1 u_1 + \dot{\theta}_{\mathrm{H}} u_2 = Mg\tan\phi\dot{X}_g. \tag{32}$$

We then face the problem of how to determine u_1 and u_2 for gait generation in real time. Using Eq. (32) to determine the control inputs, we obtain the restored mechanical energy yield constant

$$\Delta E = Mg\tan\phi\Delta X_g = 2Mlg\tan\phi\sin\frac{\theta_{\mathrm{H}}^*}{2}, \tag{33}$$

where $\Delta X_g := X_g(T^-) - X_g(0^+)$ (m) is the change in X_g for one step.

We first synthesize the desired trajectory for the hip-joint angle. To obtain smooth hip-joint motion, we developed a fifth-order time-dependent function

$$\theta_{\mathrm{Hd}}(t) = \begin{cases} a_5t^5 + a_4t^4 + a_3t^3 + a_0 & (0 \le t < T_{\mathrm{set}}) \\ \theta_{\mathrm{H}}^* & (t \ge T_{\mathrm{set}}) \end{cases}. \tag{34}$$

The coefficients a_i are set so that the following boundary conditions are satisfied:

$$\ddot{\theta}_{\mathrm{Hd}}(0) = 0,\ \dot{\theta}_{\mathrm{Hd}}(0) = 0,\ \theta_{\mathrm{Hd}}(0) = -\theta_{\mathrm{H}}^*,$$
$$\ddot{\theta}_{\mathrm{Hd}}(T_{\mathrm{set}}) = 0,\ \dot{\theta}_{\mathrm{Hd}}(T_{\mathrm{set}}) = 0,\ \theta_{\mathrm{Hd}}(T_{\mathrm{set}}) = \theta_{\mathrm{H}}^*.$$

They are given by

$$\begin{bmatrix} a_5 \\ a_4 \\ a_3 \end{bmatrix} = \begin{bmatrix} T_{\mathrm{set}}^5 & T_{\mathrm{set}}^4 & T_{\mathrm{set}}^3 \\ 5T_{\mathrm{set}}^4 & 4T_{\mathrm{set}}^3 & 3T_{\mathrm{set}}^2 \\ 20T_{\mathrm{set}}^3 & 12T_{\mathrm{set}}^2 & 6T_{\mathrm{set}} \end{bmatrix}^{-1} \begin{bmatrix} 2\theta_{\mathrm{H}}^* \\ 0 \\ 0 \end{bmatrix}; \tag{35}$$

$a_0 = -\theta_{\mathrm{H}}^*$. The desired settling time T_{set} is chosen empirically. We assume that the settling-time condition is always satisfied, as mentioned above.

We synthesize the output following control using hip-joint torque u_2 for $u_1 = 0$. We divide the control input vector in Eq. (10) to form

$$\boldsymbol{S}\boldsymbol{u} = \begin{bmatrix} 1 \\ 0 \end{bmatrix} u_1 + \begin{bmatrix} 1 \\ -1 \end{bmatrix} u_2 =: \boldsymbol{S}_1 u_1 + \boldsymbol{S}_2 u_2 \tag{36}$$

and use θ_{H} as the system's control output. If we set $u_1 = 0$, the second-order derivative of θ_{H} with respect to time is

$$\ddot{\theta}_{\mathrm{H}} = \boldsymbol{S}_2^{\mathrm{T}}\ddot{\boldsymbol{\theta}} = \boldsymbol{S}_2^{\mathrm{T}}\boldsymbol{M}^{-1}(\boldsymbol{S}_2 u_2 - \boldsymbol{C}\dot{\boldsymbol{\theta}} - \boldsymbol{g}). \tag{37}$$

We can then formulate u_2

$$u_2 = \left(\boldsymbol{S}_2^{\mathrm{T}}\boldsymbol{M}^{-1}\boldsymbol{S}_2\right)^{-1}\left(\bar{u} + \boldsymbol{S}_2^{\mathrm{T}}\boldsymbol{M}^{-1}\left(\boldsymbol{C}\dot{\boldsymbol{\theta}} + \boldsymbol{g}\right)\right), \tag{38}$$

$$\bar{u} = \ddot{\theta}_{\mathrm{Hd}} + k_{\mathrm{d}}(\dot{\theta}_{\mathrm{Hd}} - \dot{\theta}_{\mathrm{H}}) + k_{\mathrm{p}}(\theta_{\mathrm{Hd}} - \theta_{\mathrm{H}}), \tag{39}$$

where k_{p} and k_{d} are the PD gain, and are positive constants, respectively.

By substituting u_2 determined by Eq. (38) into Eq. (32), we obtain the ankle-joint torque

$$u_1 = \frac{Mg\tan\phi\dot{X}_g - \dot{\theta}_{\mathrm{H}}u_2}{\dot{\theta}_1}. \tag{40}$$

We assume $\dot{\theta}_1 > 0$ and the foot length is sufficiently long to satisfy the zero moment point (ZMP) limitation.

Figure 6 shows the simulation results for VPDW with constraint control of impact posture and $T_{\mathrm{set}} = 0.70$ (s) and $\phi = 0.02$ (rad) for the system parameter settings in Table I. The robot started walking from the initial conditions with a steady gait at $t = 0^-$; $\theta_1 = -\theta_2 = \theta_{\mathrm{H}}^*/2$; and the angular velocities $\dot{\theta}_i^-$ were set to the value given by Eq. (19). With the VPDW model, as shown in Fig. 6(d), the total mechanical

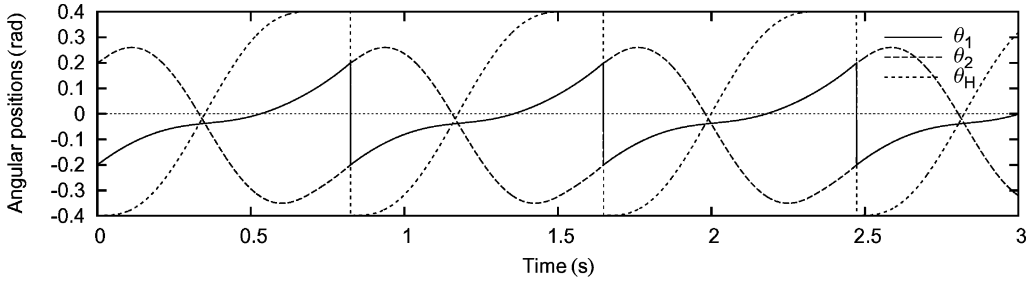

(a) Angular positions

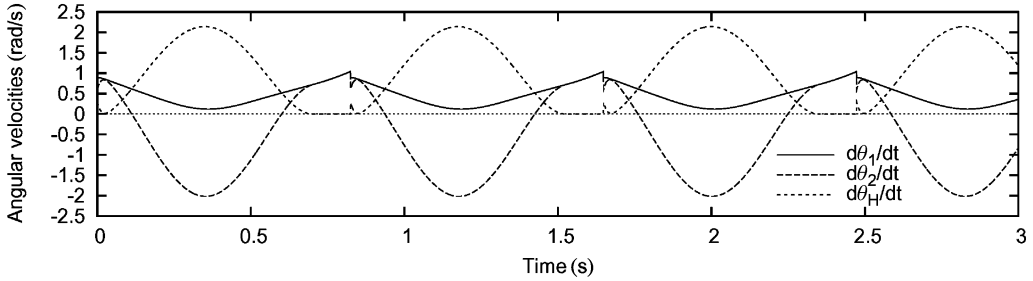

(b) Angular velocities

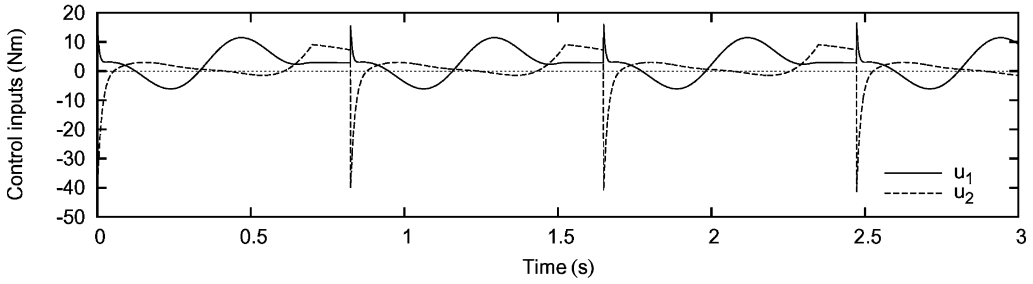

(c) Control inputs

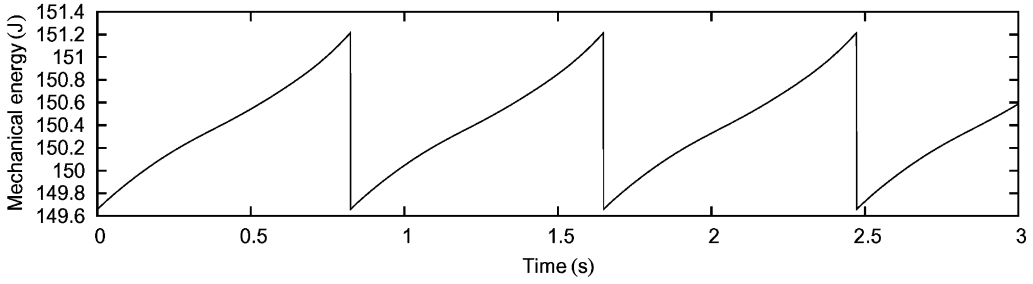

(d) Mechanical energy

Fig. 6. Simulation results for virtual passive dynamic walking with desired trajectory tracking and constraint control of hip-joint angle, where $T_{\text{set}} = 0.70$ (s).

energy was restored during single-support phases, and a stable dynamic bipedal gait was successfully generated. Figure 7 shows a stick diagram of a steady gait for one step with the feet omitted.

We next discuss gait stability. Figure 8 shows a Poincaré return map of the angular velocity immediately before impact of the stance leg $\dot{\theta}_1^-$. Several points of $\dot{\theta}_1^-[i+1]$ were numerically calculated starting from $\dot{\theta}_1^-[i]$, which is close to the equilibrium point. The stable equilibrium point is indicated at the central position. These results show that the generated gait was asymptotically stable around the equilibrium point.

7.2. On ZMP and energy efficiency

Here, we comment on the ZMP limitation and energy efficiency.

7.2.1. ZMP limitation. Satisfying the ZMP limitation is a critical problem in applying a control law to a biped robot. We must determine how the ZMP behaves in accordance

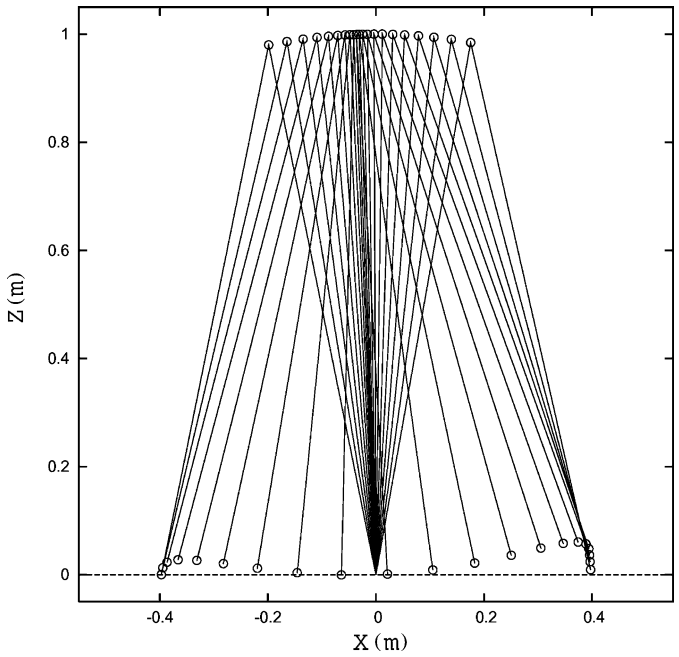

Fig. 7. Stick diagram for steady gait.

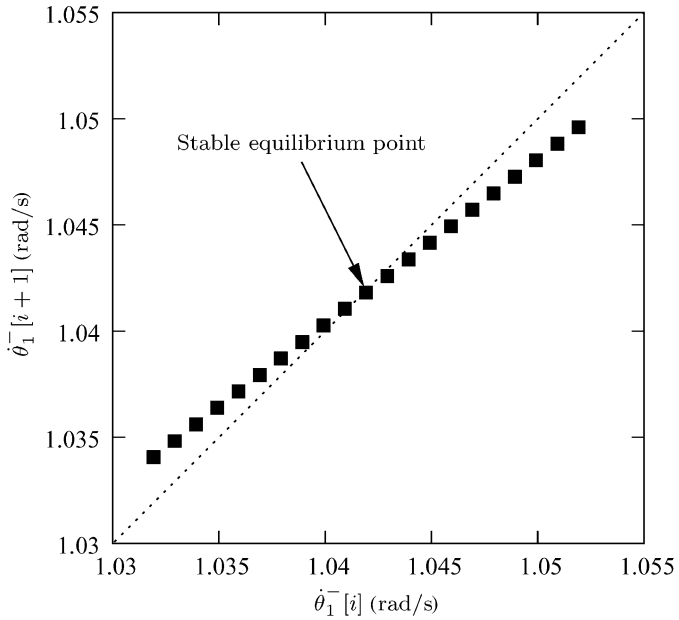

Fig. 8. Poincaré return map around stable equilibrium point.

with the control law prior to implementation. The feet must be sufficiently long so that the ZMP is not over the tilt-limitation point. We thus conducted a numerical simulation to determine how long the feet should be to cover the ZMP trajectory. We calculated the ZMP using

$$\mathrm{ZMP} = -\frac{u_1}{R_Z}, \tag{41}$$

where R_Z (N) is the vertical reaction force from the floor. Figure 9 shows the results. The ZMP remained in the range -0.10 to 0.04 (m), indicating that we must make the length with the heel-side of 0.10 (m) and toe-side of 0.04 (m). This is sufficiently short compared with the leg length.

7.2.2. Energy efficiency. Let v (m/s) be the average walking speed and p (J/s) be the average input power. Energy efficiency can then be evaluated using specific resistance p/Mgv (-), i.e. the expenditure of energy per unit mass and per unit length, which is a dimensionless quantity.[6] The question of how to attain energy-efficient biped locomotion rests on how to increase v while keeping p small. In VPDW, the relationship $p/Mgv \geq \tan\phi$ holds,[6] and the minimum specific resistance is achieved when the equality holds. In the simulation, we set ϕ to 0.02 (rad), so the minimum specific resistance was 0.02 (-). Numerical calculation showed that it was 0.0333 (-), so energy efficiency was not maximum. This is because negative input power occurred due to the trajectory tracking control. Nevertheless, efficiency was still sufficient.

7.3. Improved gait stability using robust energy control
From our findings, we derived a robust control law that uses a reference energy trajectory. When the walking pattern converges to a one-periodic gait, the system's total mechanical energy converges to a unique cycle that should be the reference trajectory for mechanical energy in a steady gait. It can be expressed as a function of X_g

$$E_\mathrm{d}(X_g) = E_0 + Mg\tan\phi X_g, \tag{42}$$

where E_0 is the value of the mechanical energy at $X_g = 0$. In steady-gait of VPDW, E_0 can be analytically determined

$$E_0 = \frac{1}{2}\bar{M}^+(\dot{\theta}_*^-)^2 + P_0(\theta_\mathrm{H}^*) + Mlg\tan\phi\sin\frac{\theta_\mathrm{H}^*}{2}, \tag{43}$$

where P_0 is the potential energy at the heel strikes. Attracting mechanical energy to desired trajectory E_d improves the convergence speed of the generated gait, which indicates that robust performance of the walking system is also improved.[6] Furthermore, if $E \equiv E_\mathrm{d}$ is achieved during the stance phase,

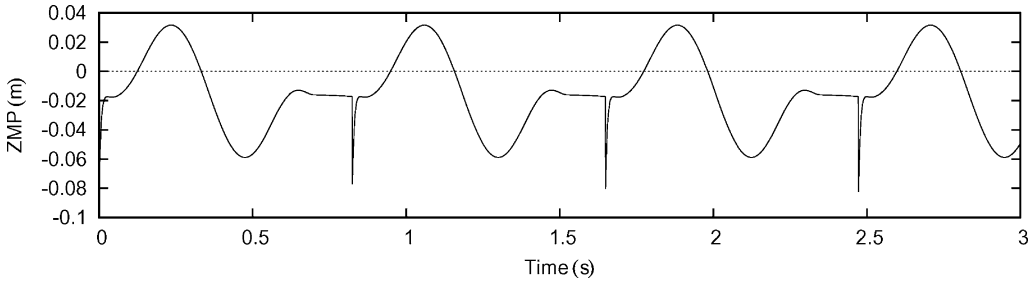

Fig. 9. Time evolution of ZMP.

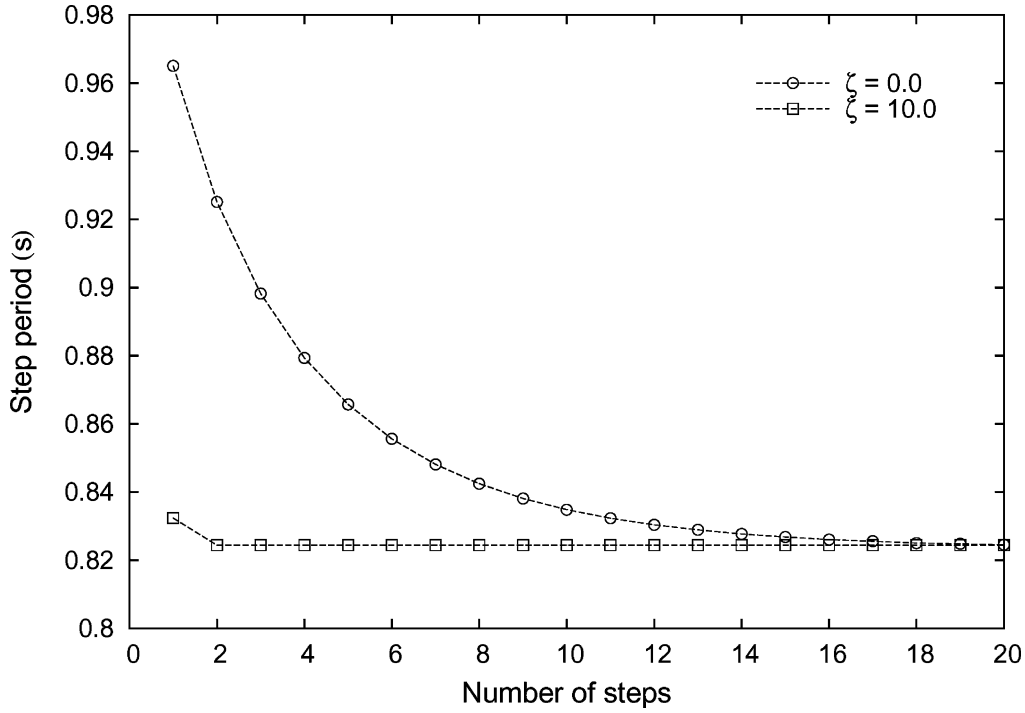

Fig. 10. Evolution of step periods in virtual passive dynamic walking with desired energy trajectory tracking control for two values of ζ.

all state variables of the constrained compass gait perfectly converge to steady ones.

We can then consider the following tracking control:

$$\frac{\mathrm{d}}{\mathrm{d}t}(E - E_{\mathrm{d}}) = -\zeta (E - E_{\mathrm{d}}), \tag{44}$$

where $\zeta \geq 0$ is the feedback gain. Combining Eq. (44) with the relationship

$$\frac{\mathrm{d}}{\mathrm{d}t}(E - E_{\mathrm{d}}) = \dot{\boldsymbol{\theta}}^{\mathrm{T}} \boldsymbol{S}\boldsymbol{u} - Mg \tan\phi \dot{X}_g, \tag{45}$$

we can formulate robust gait generation as the solution of

$$\dot{\boldsymbol{\theta}}^{\mathrm{T}} \boldsymbol{S}\boldsymbol{u} = Mg \tan\phi \dot{X}_g - \zeta (E - E_{\mathrm{d}}). \tag{46}$$

Moreover, we can solve this equation using the same algorithm described above. By substituting u_2 determined by Eq. (38) into (46), we obtain the ankle-joint torque:

$$u_1 = \frac{Mg \tan\phi \dot{X}_g - \zeta (E - E_{\mathrm{d}}) - \dot{\theta}_{\mathrm{H}} u_2}{\dot{\theta}_1}. \tag{47}$$

We must set the PD gains sufficiently large so that the mechanical energy is set to E_{d} before heel strikes. Figure 10 shows the evolution of the VPDW step period for $\zeta = 0.0$ and 10.0. The robot started walking from an initial condition close to the steady value. The effect of robust energy control is clarified by the results. When ζ was 10.0, the gait perfectly converged in one step. When it was 0.0, the generated gait was asymptotically stable.

In this method, the hip-joint torque u_2 is used for constraint control of the impact posture, and the ankle joint is driven so as to satisfy the necessary conditions for asymptotically stable gait generation in terms of making the restored mechanical energy constant. It is thus important to have enough active joints for gait stability.

8. Conclusion and Future Work

We investigated how equilibrium points are systematically determined from the mechanical energy balance point of view and found that an asymptotically stable gait can be generated based on two constraint conditions using a simple planar compass-like biped model. A robust control law utilizing the property of VPDW was derived, and its validity was confirmed by numerical simulation.

A future task is to clarify the sufficient conditions for the next impact to occur or for the potential barrier at the mid-stance to overcome. It is problematic whether or not the next impact successfully occurs. Figure 11 shows the stable domain in the T_{set}–θ^*_{H} plane for VPDW for $\phi = 0.02$ (rad). The stable area is narrow and restricted. Finding a suitable combination of T_{set} and θ^*_{H} for a given ϕ and the physical parameters is not easy without numerical testing.

We *systematically* determined the equilibrium points in a steady gait using two constraint conditions. In this sense, they are *trivial* equilibrium points. We plan to investigate the stability and robustness of general equilibrium points that are *naturally* determined without introducing any constraint conditions.

Acknowledgments

This work was partially supported by a Grant-in-Aid for Scientific Research, (B) No. 18360115, provided by the Japan Society for the Promotion of Science (JSPS).

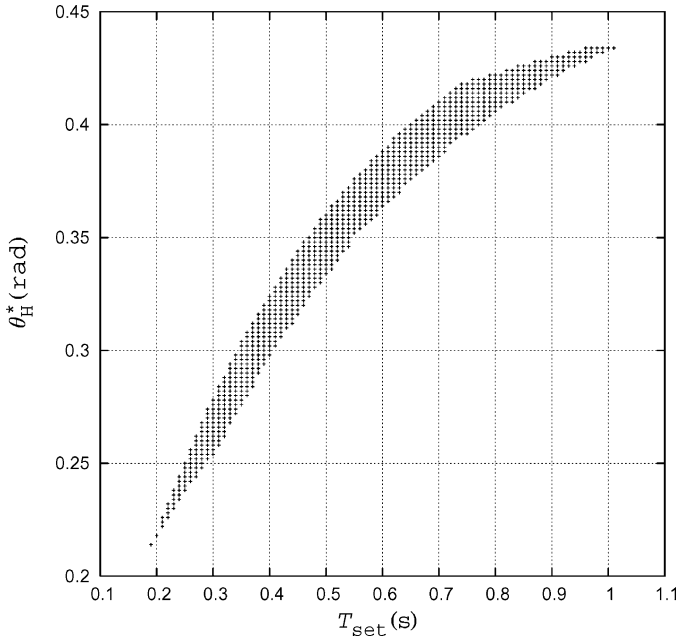

Fig. 11. Stable domain in T_{set}–θ^*_{H} plane for virtual passive dynamic walking for $\phi = 0.02$ (rad).

References

1. T. McGeer, "Passive dynamic walking," *Int. J. Rob. Res.* **9**(2), 62–82 (Apr. 1990).
2. F. Gubina, H. Hemami and R. B. McGhee, "On the dynamic stability of biped locomotion," *IEEE Trans. Biomed. Eng.* **BME-21**(2), 102–108 (Mar. 1974).
3. R. Katoh and M. Mori, "Control method of biped locomotion giving asymptotic stability of trajectory," *Automatica* **20**(4), 405–414 (Jul. 1984).
4. H. Miura and I. Shimoyama, "Dynamic walk of a biped," *Int. J. Rob. Res.* **3**(2), 60–74 (Jun. 1984).
5. A. Goswami, B. Thuilot and B. Espiau, "A study of the passive gait of a compass-like biped robot: Symmetry and chaos," *Int. J. Rob. Res.* **17**(12), 1282–1301 (Dec. 1998).
6. F. Asano, Z.-W. Luo and M. Yamakita, "Biped gait generation and control based on a unified property of passive dynamic walking," *IEEE Trans. Rob.* **21**(4), 754–762 (Aug. 2005).
7. M. Garcia, A. Chatterjee, A. Ruina and M. Colema, "The simplest walking model: Stability, complexity, and scaling," *ASME J. Biomech. Eng.* **120**(2), 281–288 (Apr. 1998).
8. S. Hosoe, K. Takeichi, S. Kumai and M. Ito, "Analysis of stability of dynamic biped locomotion with high gain feedback (in Japanese)," *Trans. Soc. Instr. Control Engineers* **22**(9), 948–954 (Sep. 1986).
9. J. W. Grizzle, G. Abba and F. Plestan, "Asymptotically stable walking for biped robots: Analysis via systems with impulse Effects," *IEEE Trans. Automat. Control* **46**(1), 51–64 (Jan. 2001).
10. Y. Ikemata, A. Sano and H. Fujimoto, "A stability mechanism of the fixed point in passive walking (in Japanese)," *J. Rob. Soc. Jpn* **23**(7), 73–80 (Oct. 2005).
11. M. Wisse, C. G. Atkeson and D. K. Kloimwieder, "Swing leg retraction helps biped walking stability," *Proceedings of the IEEE-RAS International Conference on Humanoid Robots*, Tsukuba, Japan (Dec. 2005) pp. 295–300.
12. S.-H. Hyon and T. Emura, "Symmetric walking control: Invariance and global stability," *Proceedings of the IEEE International Conference on Robotics and Automation*, Barcelona, Spain (Apr. 2005) pp. 1455–1462.
13. Y. Tazaki and J. Imura, "A study of the energy-saving effect of foot shape on planar passive bipedal walking (in Japanese)," *J. Rob. Soc. Jpn* **23**(1), 131–138 (Jan. 2005).
14. M. Coleman, "A stability study of a three-dimensional passive-dynamic model of human gait," *Ph.D. Thesis* (Cornell University, Feb. 1998).
15. F. Asano and Z.-W. Luo, "The effect of semicircular feet on energy dissipation by heel-strike in dynamic biped locomotion," *Proceedings of the IEEE International Conference on Robotics and Automation*, Roma, Italy (Apr. 2007) pp. 3976–3981.

Appendix: Energy-loss coefficient of simplest walking model

The energy-loss coefficient of Eq. (27) as a function of θ^*_{H}, β, and γ is described in detail as

$$\varepsilon(\beta, \gamma, \theta^*_{\mathrm{H}}) = \frac{N_\varepsilon(\beta, \gamma, \theta^*_{\mathrm{H}})}{D_\varepsilon(\beta, \gamma, \theta^*_{\mathrm{H}})}, \tag{A 1}$$

$$\begin{aligned} N_\varepsilon(\beta, \gamma, \theta^*_{\mathrm{H}}) = {} & 4\beta^2(\beta(\beta-1)+1) + 2\beta\gamma(\beta+1) + \gamma^2 \\ & + 4\beta(\beta-1)(\beta+\gamma)\cos\theta^*_{\mathrm{H}} + \gamma(2\beta+\gamma) \\ & \times \cos(2\theta^*_{\mathrm{H}}), \end{aligned} \tag{A 2}$$

$$\begin{aligned} D_\varepsilon(\beta, \gamma, \theta^*_{\mathrm{H}}) = {} & (2 + 2\beta(\beta-1) + \gamma + 2(\beta-1)\cos\theta^*_{\mathrm{H}}) \\ & \times (1 + 2\beta^2 + 2\gamma - \cos(2\theta^*_{\mathrm{H}})). \end{aligned} \tag{A 3}$$

By setting $\beta = 0$ and $\gamma \to \infty$, we can obtain the value of the simplest walking model. Only if $\gamma \to \infty$ is set, however, does ε uniquely converge to $\cos^2\theta^*_{\mathrm{H}}$ regardless of β. If α is constant, the restored mechanical energy ΔE yields a constant value of Eq. (4). In addition, in the simplest walking model, the leg swinging immediately before impact does not affect the state variables immediately after impact,[7] and so the constraint control of the impact posture is not necessary to keep ε constant.